Online ISSN 1848-3380, Print ISSN 0005-1144
ATKAFF 56(1), 91–99(2015)

Ivan Marinović, Duje Čoko

Inter-Floor Wide Band Radio Channel Measurements and Simulation Applying Saleh-Valenzuela Model

DOI 10.7305/automatika.2015.04.643
UDK 621.371.3.018.424.092:692.5; 519.876.5

Original scientific paper

This paper explores the accuracy of Saleh-Valenzuela (SV) statistical simulation model in time of arrival domain (ToA) applied on inter-floor wide band indoor radio channels. In order to extract the model parameters, an extensive measurement campaign was performed inside a modern building by applying vector network analyzer method at frequency of 1.8 GHz. The measurement results are presented in form of path loss exponent and delay spread statistics for each number-of-floors (NOF) distance between the antennas (up to 4). Path loss exponent was found to be around 3 for antennas on a same floor and around 5.5 for any other case when antennas were on separated floors. CDFs of rms delay spread may be divided into two groups: the first group is made of single-floor (SF) case and distanced-floors (DF) cases (three or more floors separated antennas) which showed similarities performing median value at 20 ns. For neighboring-floors (NF) cases (one and two floors separation) this value was increased to 35 ns. SV simulation, run with the extracted parameters, assessed delay spread statistics sufficiently good for the first group of CDFs. In order to assess the second group results, it was necessary to introduce simple corrections in SV model application.

Key words: Inter-floor wide band radio channel, Multipath propagation, Path loss, RMS delay spread

Simulacija radijskog kanala između katova primjenom SV modela. U radu se analizira mogućnost primjene Saleh-Valenzuelovog (SV) statističkog modela simulacije radijskog kanala u domeni kašnjenja na širokopojasne radijske kanale u zatvorenim prostorima koji obuhvaćaju više katova. Da bi se došlo do parametara simulacije, provedena je kampanja mjerenja unutar jednog objekta tipične moderne arhitekture primjenjujući metodu mjerenja s vektorskim mrežnim analizatorom na frekvenciji 1.8 GHz. Rezultati mjerenja predstavljeni su u obliku eksponenta gubitaka i kumulativne raspodjele vjerojatnosti (CDF funkcije) u ovisnosti o broju katova koji dijele odašiljač i prijamnik (do 4). Izmjereni eksponent gubitaka kretao se oko 3 za kanale na istom katu i oko 5.5 za kanale kod kojih su antene bile raspoređene na različitim katovima. Dobivene CDF funkcije mogu se podijeliti u dvije grupe: prvu grupu čine kanali na istom katu (SF) i kanali među udaljenim katovima (DF – tri ili više katova udaljene antene), koji su pokazali velike sličnosti te se mogu okarakterizirati prosječnim kašnjenjem od oko 20 ns. Za kanale između susjednih katova (NF – jedan ili dva kata udaljene antene) ova vijednost povećana je na oko 35 ns. SV simulacija, pokrenuta s izmjerenim parametrima predvidjela je CDF funkcije zadovoljvajuće dobro samo za prvu grupu kanala. Da bi se uspješno mogli simulirati i kanali iz druge grupe, predstavljen je jednostavan korekcijski model koji to omogućava.

Ključne riječi: širokopojasni radijski kanal između katova, višestazna propagacija, gubici propagacije, efektivno raspršenje kašnjenja

1 INTRODUCTION

Usual practice in the process of introducing new mobile services is to start with a detailed system scan, generating a good base of measurement data which depicts the situation in reality. According to the first image, theoretical or empirical models are being developed in order to obtain a powerful tool for prediction of system behavior in similar situations. This means that the measurement techniques and their accuracy have a crucial importance on development of simulation models because they are generally being taken as references. Mobile networks suffer of instability, generally produced by phenomenon of multipath propagation. They are well investigated and statistically described, especially for specific environments like urban areas, microcells, large building interiors, etc. Regarding the indoor environments, wireless networks are consisted of more mutually connected single-floor networks. Disposition and orientation of antennas are intended to minimize the inter-floor propagation so that inter-floor compo-

nents, even if they exist, act only as an undesirable interference. Furthermore, wide band indoor networks are mostly planned as short range networks, which means that they are designed for single-floor applications. However, some applications are intended to be of an inter-floor character, but in these cases they are rather simple and narrow-banded. Still, characterization of inter-floor wide band radio channels is a permanent task for lot of authors.

Radio channel modeling basics are well described in literature [1], [2]. Pioneer steps have been done by Turin and Guns. Turin's approach was adopted and developed by Saleh and Valenzuela [3], and their model actually presents a widely accepted statistical radio channel modeling tool.

Inter-floor propagation was much less analyzed. In [4]-[6] authors deal with physical mechanisms of an inter-floor propagation providing empirical assessments of path loss. In [7] the uniform theory of diffraction (UTD) method has been applied in order to determine site-specific wide band radio channel responses from the neighboring floors. The same deterministic method has been employed in [8] to determine the path loss characteristics between numerous floors, considering the wave polarization among other parameters. In [9] authors employ complex 3D finite-difference time-domain (FDTD) method in order to assess the inter-floor wide band channel impulse response.

The main scope of this paper is to validate the applicability of the well established Saleh-Valenzuela channel model for simulation of inter-floor radio channels just like it works for simulation of single floor channels. In order to obtain the reference values, we made a measurement campaign inside our university building. Vector network analyzer (VNA) method was applied to capture the channel impulse responses from distanced floors. Central frequency was 1.8 GHz with 400 MHz frequency span and with 150 dB of dynamic range. Our system provided sufficiently good responses from four floors distanced transmitting and receiving antenna (i.e. the third and seventh floor).

After a brief theoretical description in the second chapter, in third one the measurement setup is presented in detail. Next chapter presents the obtained results which may be characterized as rather unexpected in a way that there are some differences between two types of inter-floor radio channels. The first type includes SF and DF channels, while the second one includes NF channels. Based on these results we tried to propose procedure for application of Saleh-Valenzuela statistical method as a tool for simulation of both channel types. Sixth chapter offers the discussion about acquirements. Entire work is reviewed in Conclusion.

2 DEFINITIONS

Wide band radio channel power delay profile $P_h(\tau)$ obtained by measurements may be transformed to the channel impulse response $h(\tau)$ from [1], [2]:

$$P_h(\tau) = 10 \log h^2(\tau), \tag{1}$$

where τ stands for absolute time. Multipath power gain is:

$$G = \int_0^\infty h^2(\tau) d\tau, \tag{2}$$

mean propagation delay is:

$$\bar{\tau} = \frac{\int_0^\infty \tau h^2(\tau) d\tau}{\int_0^\infty h^2(\tau) d\tau} \tag{3}$$

rms delay spread is:

$$\tau_{rms} = \sqrt{\frac{\int_0^\infty (\tau - \bar{\tau})^2 h^2(\tau) d\tau}{\int_0^\infty h^2(\tau) d\tau}} \tag{4}$$

and wide band path loss is:

$$PL[dB] = 10 \log(G) \tag{5}$$

Path loss is generally presented in form of relative path loss PL_{rel} according to:

$$PL_{rel}[dB] = PL_0[dB] + n \cdot 10 \log(\frac{d}{d_0}) \tag{6}$$

where PL_0 stands for path loss at reference distance d_0, n is the path loss exponent, representing the channel attenuation characteristic (2 for free space). One may notice that channel characteristics strongly depend on the applied threshold level which has to be chosen in a way to achieve as great as possible system dynamics. This threshold level also defines the time of first arrival, and consequently shifts the entire profile relatively on time scale.

The same channel may be statistically simulated with the discrete model:

$$h(\tau) = \sum_k \alpha_k e^{j\theta_k} \delta(\tau - \tau_k) \tag{7}$$

where α_k, θ_k and τ_k are the amplitude, phase and relative delay of k-th ray, respectively, and $\delta(\tau)$ is the Dirac function. The equivalent parameters may be calculated with:

$$G = \sum_i \alpha_i^2(\tau) \tag{8}$$

$$\bar{\tau} = \frac{\sum\limits_i \tau_i \alpha_i^2}{\sum\limits_i \alpha_i^2} \tag{9}$$

$$\tau_{rms} = \sqrt{\frac{\sum\limits_i (\tau_i - \bar{\tau})^2 \alpha_i^2}{\sum\limits_i \alpha_i^2}} = \sqrt{\bar{\tau^2} - (\bar{\tau})^2} \tag{10}$$

The rule for generation of rays is defined by some simulation model, generally characterized by the model parameters. The same procedure should be applied on processing of simulated profiles, involving the same threshold level and time window. Model parameters should be determined to achieve the best possible agreement between measured and simulated cumulative distribution functions (CDFs) of rms delay spread as well as between path loss exponents. Having a powerful simulation tool, it is possible to obtain channel characteristics for a distant new environment simply by adapting the model parameters, but with no necessity for new measurements.

3 MEASUREMENT PROCEDURE

Three methods may be applied to determine the channel impulse response: RF-impulse method, VNA-method and PN-sequence method [1], [2]. In [10], [11] the vector network analyzer method is explained in detail.

The main task of the measurement setup synthesis was to achieve as high as possible system dynamics, since the inter-floor rays have to pass through reinforced concrete floors, experiencing high attenuation. We applied vector network analyzer method as the most frequently used method for indoor channel scanning. The general practice is to connect the receiving antenna directly to the VNA's port 2 in order to avoid superposition of additional noises to weak received signals, which may happen if additional amplifiers are used. This fact limits the "down-side" of the dynamic range to around -90 dBm which characterizes our VNA HP 8720A. "Up-side" of the dynamic range is limited with maximal transmitted power which we chose to be 30 dBm (1 W). Such arranged system provided 120 dB of dynamic range which was additionally increased to 140 dB by applying the averaging function of the VNA. Transmitter side of the VNA (port 1) started with -10 dBm signal level which is the maximal output level of the VNA. The open loop gain had to be 40 dB, matching with 30 dBm transmitted power. We intended to explore channel characteristics on relatively long distances for indoor propagation, which needed long cables to be applied. Cable loss had to be compensated by addition of amplifiers, having in mind a total gain of 40 dB. Our assessment was that cable length of 80 m may suit all our needs. The chosen cable type was RG58/U with 0.9 dB/m loss at 1.8 GHz making the total section loss 70 dB. This means that gain of the amplifiers chain had to be 110 dB. Applying the cable as a single piece, the signal level would have dropped to an extremely low level of -80 dBm. Because of that, we divided the cable into three sections, while amplification of 110 dB was achieved using four amplifiers. Fig. 1. presents the measurement setup with list of applied cables and amplifiers in Table 1.

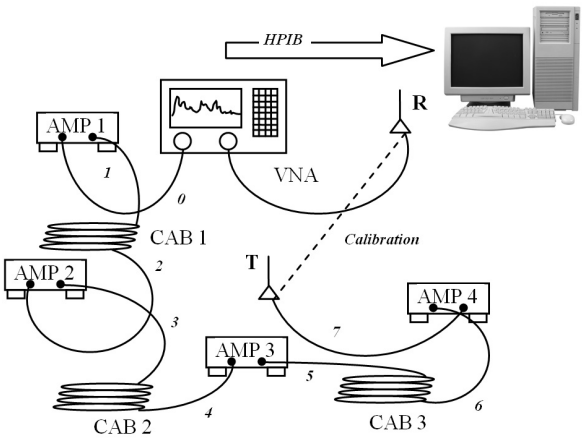

Fig. 1. Measurement system

Table 1. List of applied cables and amplifiers

	Gain (dB)	Type
CAB 1	-20	RG58/U
CAB 2	-25	RG58/U
CAB 3	-15	RG58/U
AMP 1	15	Miteq linear pre-amplifier
AMP 2	35	Miteq linear pre-amplifier
AMP 3	30	Miteq linear pre-amplifier
AMP 4	30	HP 489A power amplifier 1W

Applying this scheme the lowest signal level along the system (points 0 through 7) was -25 dBm at point 2. This measurement system needed addition of 10 dB linear attenuator in order to be calibrated. Namely, transmitted power was set to 30 dBm, while the maximal input power of the VNA is 20 dBm. The attenuator had to be connected in series with calibration "thru" element, but we decided to use the internal attenuator of AMP4, avoiding additional error of electrical length of the attenuator. We checked the linearity of the amplifier's attenuator which performed as excellent. When calibration was finished, the attenuator had to be returned on previous level and obtained results should have been corrected for 10 dB (subtracted from a power delay profile (PDP)). We took a special attention

to the choice of antennas due to the fact that their omni-directional characteristics in H-plane have a crucial role for the accuracy of the results. Furthermore, regarding the fact that we scanned multi-floor radio channels, even vertical characteristics in E-plane should be considered because antennas operated with high elevation angles. The list of applied antennas with their characteristics may be found in Table 2.

The antennas were mounted on non-metallic stands at height of 1 m. AMP 4 and VNA were positioned close to the transmitting or receiving antenna, but in a way not to influence the measurement results (under their respective antennas).

Central frequency was 1800 MHz with frequency sweep of 400 MHz. This resulted in the system time resolution of 2.5 ns or spatial resolution of 0.75 m. With 800 points per measurement, the time window of 2 μs was achieved. Wavelength at central frequency was 17 cm. The VNA was equipped with direct time domain transform function where a normal windowing function was applied to the measured results. The data was transferred into the computer through HPIB cable.

4 ANALYSIS OF THE RESULTS

4.1 Frequency band and measurement technique

The most frequently used indoor networks are GSM and Wi-Fi networks in the frequency bands of 0.9/1.8/2.4GHz. Our principal intention was to collect one propagation data set, but in a way that conclusions may be taken more widely. Having in mind that parameters of construction materials do not change significantly inside mentioned frequency range, we chose frequency of 1.8 GHz as a center frequency for measurements. Furthermore, VNA-method means frequency sweep inside defined frequency span (which we chose to be 400 MHz) enforcing our decision.

The measurements were performed inside our FESB-University building during non-business periods to avoid the influence of people and machines. We intended to obtain as 'clear' as possible channel image in order to detect principal propagation phenomena, presuming that all additional influences may simply be involved in statistical analysis afterwards. The receiving antenna and VNA were located on the fifth floor, while the amplifiers and transmitting antenna were mobile. We scanned the fifth floor and four under-floors and four upper-floors, even though the geometry was too complex for upper-floor cases. Results from symmetrical floors (i.e. one floor up and one floor down) were put into the same data set. Therefore, data from five levels were obtained. At each floor, we took data on at least eight random locations. At each location we made nine measurements, following the rectangular grid

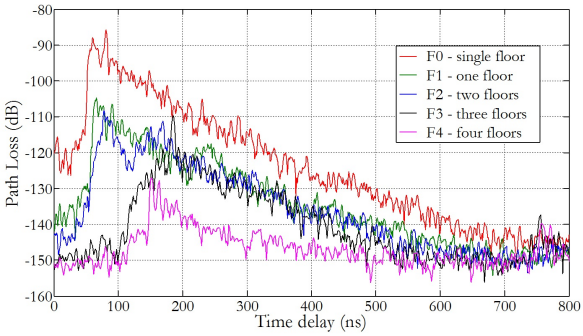

Fig. 2. Samples of power delay profiles between floors

of 10 cm by 10 cm in order to obtain spatially averaged profiles [12], [13], [14]. Time averaging was achieved by switching on the averaging function of the VNA (last 16 measurements).

4.2 Power delay profiles

Sample results of the measurements are presented on Fig. 2. We chose one spatially and time averaged profile for every NOF distance to represent the channel 'image'. The profiles are randomly chosen so that the time of first arrival for each PDP depends on location of the transmitting antenna on the sample floor. We succeeded to obtain PDPs from five floors separated antennas which means that, with the receiving antenna located on the fifth floor, the transmitting antenna was positioned either on the ground level or on the tenth floor. Unfortunately, in case of five floors distanced antennas, the peak value on the PDP was only about 7 dB above the noise level which was not sufficient for statistical analysis so that this profile is not presented on the figure. The system noise level is about -90 dBm which matches with path loss noise floor of -150 dB, which is 10 dB more optimistic than our assessment. The reason for this is that we made a worst case design of the signal attenuation, always taking rounded values. One may see that the propagation path loss increases with NOF distance. PDP for single floor propagation is the least attenuated, but PDPs for one, two and three floors distanced antennas remain approximately equally attenuated. Finally, four floors distanced antennas are additionally attenuated. It has to be said once again that these profiles are only the examples of a lot of measured profiles.

4.3 Path loss analysis

Arranging the path loss of all measured groups of profiles according to (6) we obtained the results presented on Fig. 3. Graphs for path loss exponent n resulted as a linear best fit approximation of measured results. This analysis applied on single floor case yields value of 44.4 dB for reference path loss although Friis equation gives 37.6 dB.

Table 2. Antennas' characteristics

Antenna	Make/Model	Gain (dB)	HPBW (deg)	Frequency range (MHz)	Power/Sensitivity
Transmitter Dual Discone-type	A-info JXTXSZ-50300/P	0	40	50 – 3000	100W / -
Receiver Conical Dipole	Seibersdorf Research PCD 8250	0	85	80 – 3000	0.1W

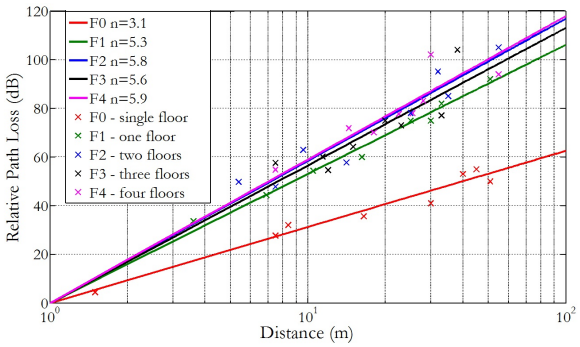

Fig. 3. Path loss exponents

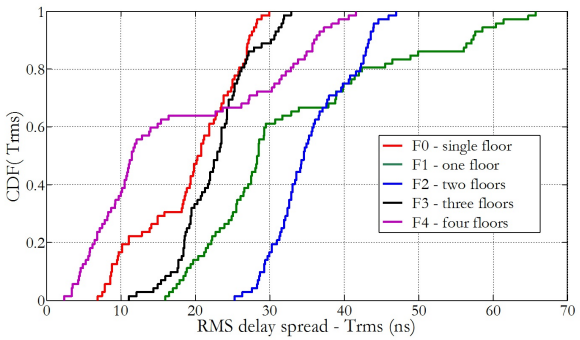

Fig. 4. Rms delay spread of inter-floor radio channels

Parameter n gets a value of 3.1 for single floor case and values between 5.3 and 5.9 for all other cases. Path loss exponent n with associated rms fitting error for each floor is presented in Table 3.

4.4 Rms delay spread statistics

Regarding the rms delay spread, definition of threshold level plays a crucial role for accuracy of the results. We chose to keep a constant path loss threshold level of -140 dB which corresponds with noise floor of -90 dBm. This ensures the maximal possible dynamic range, which varied from about 10 dB up to about 50 dB. Results are presented graphically on Fig. 4. and numerically in Table 4. (min stands for minimal value, max for maximal, mean for mean, med for median and std for standard deviation). Results partially disagree with some reported in literature [2], [13], but they characterize a 'slightly-echoic' environment. Distribution functions are relatively spread, but two groups may be recognized. Single-floor case (F0), three-floors (F3) and four-floors (F4) cases are characterized with smaller delay spread compared with one floor (F1) and two floors (F2) cases. For this reason, we decided to form two new distributions which will consist of data from F0, F3 and F4 cases as well as of data from F1 and F2 cases. These new distributions are marked as F0F3F4 and F1F2 distributions, Table 4. and Fig. 5. They have very similar shape with variances of 9 ns and 10 ns, respectively, but with mutual time shift of about 15 ns. These distributions will be taken as the proposed distributions for further analysis because they are typical and represent all

Table 4. Statistical properties of single-floor and inter-floor radio channels

[ns]	min	max	mean	med	std
F0	7.50	30.00	19.25	20.25	6.69
F1	17.00	64.70	32.94	28.35	13.42
F2	25.30	47.00	35.23	34.25	5.53
F3	12.10	32.90	22.74	22.50	4.88
F4	2.40	41.60	17.34	11.00	12.66
F0F3F4	2.40	41.60	19.78	20.30	8.94
F1F2	17.00	64.70	34.09	32.50	10.25

propagation scenarios. For the simplicity, we gave them names single floor - distanced floors distribution (SFDF) and neighboring floors distribution (NF). The first one relates to F0F3F4 distribution and second one to F1F2 distribution.

4.5 Small scale fading statistics

As the final step, it was necessary to explore the small-scale fading characteristics of the local field strength. We analyzed the normalized voltage path gain for each spatially averaged profile and for all NOF-distances separately. The general trend is that, for a given floor, practically at any point of measurements we obtained very similar field statistics. Moreover, there is no significant difference in field statistics along the NOF-distance. Rayleigh and Log-normal distributions performed the best fit to the normalized voltage path gain CDFs. Fig. 6. and Fig. 7. present the results for F0 and F4 case separately. The values in brackets are the maximum likelihood estimations for

Table 3. Fitting results for path loss exponents

NOF distance	0	1	2	3	4
Path loss exp. n	3.1	5.3	5.8	5.6	5.9
RMS error ϵ (dB)	2.0564	2.9647	6.6798	5.2496	3.6068

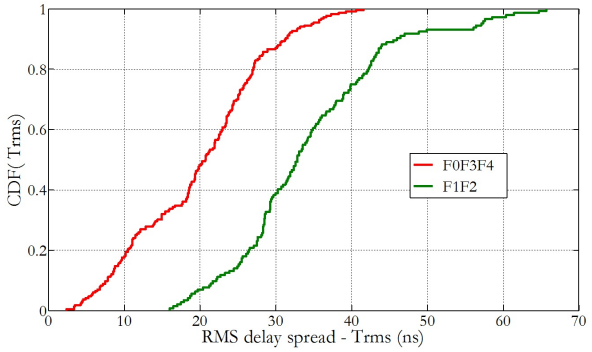

Fig. 5. Proposed CDFs for SFDF (F0F3F4) and NF (F1F2) propagation

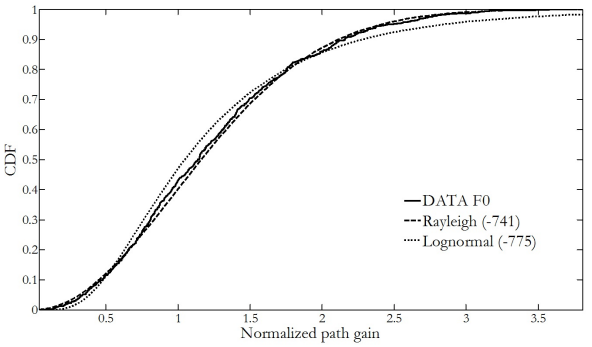

Fig. 6. CDFs of normalized path voltage gain for F0 case

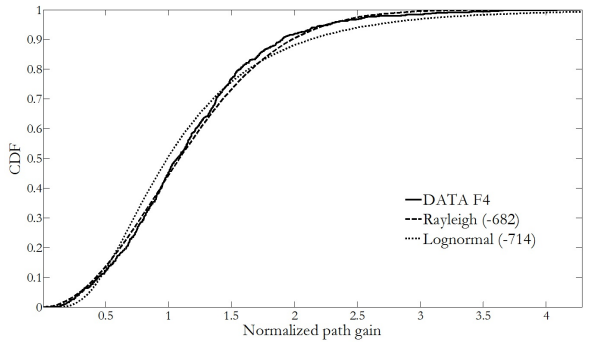

Fig. 7. CDFs of normalized path voltage gain for F4 case

the respective distribution fits.

5 SIMULATION OF PROPAGATION

According to the authors [3], radio channel may be simulated by the discrete time model. It states that rays arrive to receiver in clusters which is the consequence of reflections from large scatterers present inside the environment. Channel impulse response may be statistically modeled with certain number of clusters of rays (N_{cl}) whose exact number for defined profile should be picked from the Poisson distribution. Number of rays inside each cluster is also from Poisson distribution with another parameter (N_{ra}). Clusters appear with defined frequency ($1/\Lambda$), but exact inter-arrival times between clusters should be picked from the exponential distribution with the same parameter (Λ). The equal rule stands for rays inside the clusters, with different ray frequency ($1/\lambda$). Power gains of first rays inside the clusters should follow decaying exponential rule with constant Γ, as well as power gains of rays inside clusters with another constant (γ). Finally, each ray as a path power gain should be picked from exponential distribution which meets with Rayleigh distribution of path voltage gains. The problem is positioned relatively which means that rms delay spread may be calculated by taking normalized values of path power gains. Their exact values may be determined using the path loss exponent n obtained by measurements [5]. Every simulated power delay profile has to be limited with time window (T_w) and with threshold level (P_{thresh}). RMS delay spread should be calculated for every simulated delay profile, so that repeating the process for great number of profiles, the CDF of rms delay spread can be determined.

The first observations on all measured PDPs show that there are no significant differences between them. But, taking a closer look at the profiles, it is obvious that there are some differences between the SFDF and NF profiles. Namely, SFDF profiles follow general trend of linearly decaying cluster amplitudes (in dB) while this does not stand for NF profiles. In those cases clusters appear with random amplitudes, but also disappearing with time. A good example for this behavior may be found on Fig. 2. PDP for F2 case (blue line) exhibits second cluster practically equal with the starting cluster. Here rises a question, is it possible to simulate even these channels using the SV model and how to extract the model parameters. In that case, it is obvious that the only difference should be in values of decaying constants Γ and γ. So, as a first step we decided to extract the model parameters from SFDF profiles, Table 5. (first row) and Fig. 8. The parameters were extracted

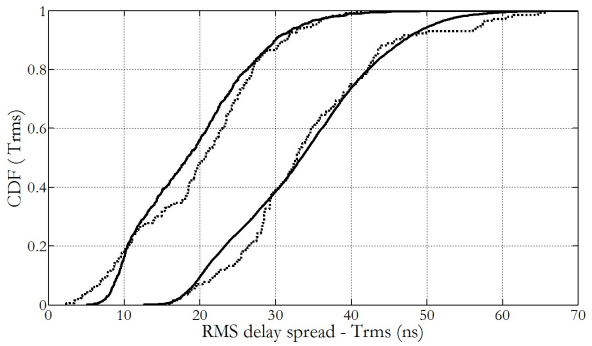

Fig. 8. Proposed CDFs simulated by Saleh-Valenzuela model

from the averaged measured profiles for certain group of profiles. These parameters are very similar to the results obtained by other authors [3], [10], [15] for measurements inside similar buildings. One may see that simulation results based on these parameters fit to measured graph sufficiently good, predicting a median value at 18 ns instead of 20 ns. In order to assess the NF graph, we optimized the values for decaying constants, Table 5. (second row) and Fig. 8. The best fit was achieved for $\Gamma = 50\ ns$ instead of 35 ns and for $\gamma = 20\ ns$ instead of 10 ns. This yielded a median value of 34 ns instead of 33 ns.

If the clusters in NF cases did not decay exponentially as in SFDF cases but following an undefined rule, as a first approximation it was reasonable to try to explain this behavior with exponential rule as well. In that case decaying constants should have been much increased, in our case almost doubled. If we propose the new relations for assessment of Γ' and γ' constants according to:

$$\Gamma' = k_1 \Gamma \tag{11}$$

$$\gamma' = k_2 \gamma \tag{12}$$

yields $k_1 = 1.43$ and $k_2 = 2$. Changing the other simulation parameters had no physical explanation neither the experimental verification.

6 DISCUSSION

It was reasonable to expect that path loss will increase with the NOF distance between the antennas, having in mind strong field attenuation due to the floors made of reinforced concrete. The results show a different trend, yielding the path loss exponent around 3 for single floor case and around 5.5 for all other cases. The reason for this behavior may be found in [4-9]. Transmitted ray is not the principal mechanism of propagation, especially not between distanced floors. This role is taken over by diffracted rays or even reflected rays through vertical apertures inside a building. In [8] our research team made an extensive analysis of propagation mechanisms applying UTD method. The particular decaying constants were proposed for transmitted, diffracted and reflected waves respectively, taking into consideration wave polarization. Their values are 6.8 through 12.1 for vertical polarization and 8.3 through 11.3 for horizontal polarization. The received signal is a vector sum of all rays which may produce smaller value for total field path loss exponent. Having in mind that direction of propagation is horizontal in the case of single floor propagation but vertical for inter floor propagation, situation becomes more complex. Incident angles are generally very high, producing cross polarization components. The consequence of all mentioned phenomena is the fact that rays do not decay in such extent as it was expected. Indeed, it seems that propagation takes place through certain number of floors as if obstacles do not exist. Naturally, this is not valid for single floor propagation where signals have minimal attenuation.

Delay spread obtained by measurements shows some interesting properties. NF cases are characterized with extended time delay of about 15 ns comparing with SFDF cases. The reason for this may be found in fact that these cases are characterized with dominant first cluster on PDP while this does not stay for NF cases. It is proven by Saleh-Valenzuela model that more clusters exist on radio channel, but thanks to the attenuation, sometimes they are overlapped and masked. That is the case in single floor situation (where direct ray cluster dominates over all other clusters) and in distanced floors situations (where direct-ray transmitted through floors practically disappears and only the diffracted-ray clusters remain). On the contrary, in the NF cases, the transmitted-ray and diffracted-ray clusters exhibit similar amplitudes, so that general trend of exponentially decaying clusters does not stand. Thanks to the longer path distance of diffracted rays, the resulting rms delay spread gets greater.

Cumulative density function of rms delay spread may be reasonably good assessed for SFDF propagation applying SV model. In order to assess the statistics for NF cases, it was necessary to adjust the model parameters. In this paper, according to explained physical mechanisms of propagation, the simple procedure for correction of model parameters for NF cases has been proposed. It assumes that exponentially decaying rule for clusters and rays amplitudes may be sustained, but with significantly increased decaying constants. Further measurements are needed to define some empirical relation or even new statistical model which would more precisely define this problem.

Table 5. Parameters for Saleh-Valenzuela simulation (SFDF - first line, NF - second line)

N_{cl}	N_{ra}	$1/\Lambda$	$1/\lambda$	Γ	γ	T_w	P_{thresh}
4	30	150ns	5ns	35ns	10ns	800ns	-140dB
4	30	150ns	5ns	50ns	20ns	800ns	-140dB

7 CONCLUSION

The wide band inter-floor channel characteristics are being investigated. In order to obtain path loss exponent and rms delay spread characteristics for different NOF antennas separation, the wide band measurements at 1.8 GHz band are performed inside typical modern building. System dynamics of about 150 dB provided power delay profiles for antennas separated up to four floors.

Analysis of the results shows that signal power decays while moving the antenna upstairs or downstairs through the building, but very slightly. This is the consequence of phenomenon of diffraction through windows, which provides practically equal field strength at any floor. Regarding the rms delay spread, it is similar to the results proposed from other authors, but only in the cases where one cluster dominates over all others. That is the case for propagation on single floor and for propagation where antennas are separated three or more floors (we introduced term single floor and distanced floors propagation - SFDF). In the cases of one and two floors distanced antennas (we introduced term neighboring floors propagation - NF) the transmitted and diffracted rays simultaneously take role on propagation path, but with much greater delay of diffracted rays. Simulation of inter-floor propagation is possible by applying the standard Saleh-Valenzuela model for propagation through single floor. For the neighboring floors propagation cases, the parameter values should be corrected according to proposed rule. The obtained model parameters may be applied for simulation of propagation inside similar objects. The exact rule for parameters adaptation still has to be determined, but it is clear that physical dimensions of the building and applied materials will have a strong impact on it. Greater dimensions will decrease the cluster frequency, while highly reflective internal walls will increase the decaying constants. The conclusions call for further work in the wide band inter-floor radio channel modeling.

REFERENCES

[1] R. Steele, Mobile Radio Communications. London, England; Pentech Press Limited, 1992.

[2] H. Hashemi, "The Indoor Radio Propagation Channel," Proc. IEEE, Vol. 81, no. 7, pp. 943-968, 1993.

[3] A.A.M. Saleh, R.A. Valenzuela, "A Statistical Model for Indoor Multipath Propagation," IEEE J. Sel. Areas Commun., Vol. 5, no. 2, pp. 128-137, 1987.

[4] W. Honcharenko, H. L. Bertoni, J. Dailing, "Mechanisms Governing Propagation Between Different Floors in Buildings," IEEE Trans. Antennas Propag., Vol. 41, no. 6, pp. 787-790, 1993.

[5] S. Y. Seidel, "914 MHz Path Loss Prediction Models for Indoor Wireless Communications in Multifloored Buildings," IEEE Trans. Antennas Propag., Vol. 40, no. 2, pp. 207-217, 1992.

[6] K.-W. Cheung, J. H.-M. Sau, R. D Murch, "A New Empirical Model for Indoor Propagation Prediction," IEEE Trans. Veh. Technol., Vol. 47, no. 3, pp. 996-1001, 1998.

[7] S. Y. Tan, M. Y. Tan, H. S. Tan, "Multipath Delay Measurements and Modeling for Interfloor Wireless Communications," IEEE Trans. Veh. Technol., Vol. 49, no. 4, pp. 1334-1341, 2000.

[8] Marinovic, I. Zanchi, Z. Blazevic, "On the Inter-Floor Radio Propagation: General UTD Analysis," Int. Rev. Phy., Vol. 3, no. 2, pp. 135-142, 2009.

[9] C. M. Austin, M. J. Neve, G. B Rowe, "Modelling Propagation in Multi-Floor Buildings using the FDTD Method," IEEE Trans. Antennas Propag., Vol. 59, no. 11, pp. 4239-4246, 2011.

[10] M. Sanchez Varela, M. Garcia Sanchez, "RMS Delay and Coherence Bandwidth Measurements in Indoor Radio Channels in the UHF Band," IEEE Trans. Veh. Technol., Vol. 50, no. 2, pp. 515-525, 2001.

[11] Z. Blazevic, I. Zanchi, I. Marinovic, "Propagation Measurements at 2.4 GHz Inside a University Building and Estimation of Saleh-Valenzuela Parameters," J. Commun. Softw. Syst., Vol. 3, no. 2, pp. 99-107, 2007.

[12] T. S. Rappaport, "Characterization of UHF Multipath Radio Channels in Factory Buildings," IEEE Trans. Antennas Propag., Vol. 37, no. 8, pp. 1058-1069, 1989.

[13] R. A. Valenzuela, O. Landron, D. L. Jacobs, "Estimating Local Mean Signal Strength of Indoor Multipath Propagation," IEEE Trans. Veh. Technol., Vol. 46, no. 1, pp. 203-212, 1997.

[14] W. Honcharenko, H. L. Bertoni, J. L. Dailing, "Bilateral Averaging Over Receiving and Transmitting Areas for Accurate Measurements of Sector Average Signal Strength Inside Buildings," IEEE Trans. Antennas Propag., Vol. 43, no. 5, pp. 508-512, 2007.

[15] S. Mota, M.O. Garcia, A. Roca, F. Perez-Fontan, "Clustering of the multipath radio channel parameters," in Proceedings of the 5th European Conference on Antennas and Propagation, (Rome, Italy), pp. 3232-3236, April 2011.

Ivan Marinović was born in Split, Croatia, 1966. He received B.S. degree 1989, M.S. degree 1997 and PhD 2005 at University of Split. He is presently an Associate Professor at Department of Electronics at the same University. His fields of interest include electronic circuits, RF and microwave electronics and radiocommunications. Dr. Marinović is a member of IEEE, CCIS and KoREMA.

Duje Čoko was born in Split, Croatia in 1983. He received the B.S. degree in 2007 and PhD in 2013 at University of Split, Faculty of Electrical Engineering, Mechanical Engineering and Naval Architecture (FESB), Split, Croatia. He is presently a research assistant at the Faculty of Electrical Engineering, Mechanical Engineering and Naval Architecture (FESB). His fields of interest include electronic circuits and ultra wideband channel modeling. Dr. Čoko is a member of IEEE and CCIS.

AUTHORS' ADDRESSES

Assoc. Prof. Ivan Marinović, Ph.D.
Duje Čoko, Ph.D.
Department of Electronics,
Faculty of Electrical Engineering, Mechanical Engineering and Naval Architecture (FESB),
University of Split
Ruđera Boškovića 32, HR-21000 Split, Croatia
email: imarin@fesb.hr, dcoko@fesb.hr

Received: 2013-09-02
Accepted: 2014-10-02